Chemosphere 285 (2021) 131370

Contents lists available at ScienceDirect

Chemosphere

journal homepage: www.elsevier.com/locate/chemosphere

Energy production from treatment of industrial wastewater and boron removal in aqueous solutions using microbial desalination cell

A.Y. Goren [a], H.E. Okten [a,b,*]

[a] Izmir Institute of Technology, Department of Environmental Engineering, İzmir, Turkey
[b] Environmental Development Application and Research Center, İzmir, Turkey

ARTICLE INFO

Handling Editor: Derek Muir

Keywords:
Boron removal
Microbial desalination cell
Energy production
Geothermal brine

ABSTRACT

As a result of a much needed paradigm shift worldwide, treated saline water is being considered as a viable option for replacing freshwater resources in agricultural irrigation. Vastly produced geothermal brine in Turkey may pose a significant environmental risk due to its high ionic strength, specifically due to boron. Boron species, which are generally found uncharged in natural waters, are costly to remove using high-throughput membrane technologies such as reverse osmosis. Recent advances in bioelectrochemical systems (BES) has facilitated development of energetically self-sufficient wastewater treatment and desalination. In this study, removal of boron from synthetic solutions and real geothermal waters, along with simultaneous energy production, using the microbial desalination cell (MDC) were investigated. Optimization studies were conducted by varying boron concentrations (5, 10, and 20 mg L^{-1}), air flow rates (0, 1, and 2 L min^{-1}), electrode areas (18, 24, 36, and 72 cm^2), catholyte solutions, and operating modes. Even though the highest concentration decrease was observed for 20 mg-B L^{-1}, 5 mg-B L^{-1} concentration experiment gave the closest result to the 2.4 mg-B L^{-1} limit value asserted by WHO. Effect of electrode surface area was proven to be significant on boron removal efficiency. Employing the optimum conditions acquired with synthetic solutions, boron and COD removal efficiencies from real geothermal brine were 44.3% and 90.6%, respectively. MDC, being in its early levels of technology readiness, produced promising desalination and energy production results in removal of boron from geothermal brine.

1. Introduction

Geothermal waters can be characterized by diverse physicochemical parameters depending on the depth at which resources reside, the geological characteristics of the rocks involved, and the source of water supply. Geothermal waters contain significant amounts of cations and anions along with neutral species. Specifically, boron content is critical in geothermal waters with such high concentrations, even exceeding its levels in sea water and brackish water. The main sources of boron can be either natural such as leaching from rocks, soils containing borates and borosilicates, and volcanic activities, or industrial such as manufacturing of detergents, cleaning products, semiconductor, borosilicate glass, cosmetics, fertilizers, flame retardants and dyestuff (Kartikaningsih et al., 2016). The most common boron species in geothermal waters and boron rich thermal springs are undissociated boric acid (H3BO3) and tetrahydroxoborate ions (B(OH)4-) (Yılmaz et al., 2008). H3BO3 is the dominant species at low pH values, while B(OH)4- is dominant at high pH values (>8–9) (Barth, 2000; Kabay and Bryjak, 2015). Therefore, the pH adjustment must be applied based on the pKa value of boric acid to ionize it before treating boron containing water streams. The dissociation of boric acid as a weak acid was reported using following equations:

$$H_3BO_3 \leftrightarrow H^+ + H_2BO_3^- \quad (pKa1: 9.14) \tag{1}$$

$$H_2BO_3^- \leftrightarrow H^+ + HBO_3^{-2} \quad (pKa2: 12.74) \tag{2}$$

$$HBO_3^{-2} \leftrightarrow H^+ + BO_3^{-3} \quad (pKa3: 13.8) \tag{3}$$

In terms of environmental impacts of geothermal sources, uncontrolled discharge to environment following well tests or during regular operation pose a serious problem due to high boron content. Boron accumulates in the soil upon discharge and change the chemical, physical and biological properties of soils. Also, these waters mix with groundwater by percolating through the soil and may form complexes with heavy metals (i.e. Pb, Cu, Cd, Ni, Co), which may be more toxic than heavy metals forming them (Wuana and Okieimen, 2011).

* Corresponding author. Izmir Institute of Technology, Department of Environmental Engineerimg, İzmir, Turkey.
E-mail address: haticeokten@iyte.edu.tr (H.E. Okten).

https://doi.org/10.1016/j.chemosphere.2021.131370
Received 29 November 2020; Received in revised form 17 June 2021; Accepted 26 June 2021
Available online 28 June 2021

Consequently, boron has a significant impact on water resources and corresponding ecosystems (Gude, 2016).

Depending on concentration, boron may either support or hinder plant growth where geothermal water is used for irrigation. Deficiency of boron may result in loss of yield, reduced growth and even death (Yılmaz et al., 2008). Boron is an essential nutrient for plant growth and depending on plant type, there is a wide range of tolerance (blackberry, lemon: 0.5 mg L^{-1}; walnut, plum, pear, apple: 1 mg L^{-1}; sunflower, potato, cotton, tomato: 2 mg L^{-1}; asparagus, palm, bean, onion: 4 mg L^{-1}) (Yılmaz et al., 2008; Hilal et al., 2011). However, exposure to excess boron causes toxicity for nearly all plants. Additionally, long term ingestion of high boron concentrations through water or vegetables may lead to nausea, lethargy, diarrhea, vomiting, dermatitis, intellectual and physical problems at children and risk of miscarriage in pregnancies (Nielsen, 2002; Bryjak et al., 2008).

In order to tackle high concentrations of boron, treatment methods such as coagulation, sedimentation, filtration, adsorption, membrane filtration, ion-exchange, electrocoagulation, electrodialysis, and hybrid processes have been studied (Yılmaz et al., 2007, 2008; Banasiak and Schafer, 2009; Dominguez-Tagle et al., 2011; Al-Qodah et al., 2020; Al-Bsoul et al., 2020). However, challenges such as high operation costs, production of chemical sludge, excessive use of chemicals, membrane fouling, either individually or as a combination, hampers efficient use of these methods (Arar et al., 2013; Ozbey-Unal et al., 2018; Recepoğlu et al., 2018).

Bioelectrochemical systems (BESs) as novel water and wastewater treatment methods have drawn attention due to their lower costs and less environmental impacts. The most investigated BESs are microbial fuel cells (MFCs), which are electrochemical devices that convert chemical energy from organic substrates to electrical energy via microbially-catalyzed reactions (Logan et al., 2007; Ren et al., 2014). Microbial desalination cell (MDC) is a BES technology that is derived from MFCs by inserting an anion exchange membrane (AEM) and cation exchange membrane (CEM) bordered desalination chamber between anode and cathode chambers, respectively (Kim and Logan, 2011; Tawalbeh et al., 2020). Electrodes at anode and cathode compartments are connected through a circuit, which transfers electrons that are produced by oxidation of organic substrates in anolyte under anaerobic conditions. Oxygen as an external electron acceptor, which is provided at cathode cell, uses transferred electrons to sustain reduction and produce water. Therefore, a potential electrochemical gradient is formed across the oxidative anodic and reductive cathodic chambers, which drives the desalination process. Anions migrate from salty water in desalination cell across AEM into the anode chamber, while cations move across CEM into the cathode chamber. Migration of ions in desalination cell across the membrane based on concentration gradient through diffusion is the driving force for desalination process. In the borate form (pH > pKa), the core boron species is fully hydrated in the solution that results in a larger radius and a charge enhancement of the ions [B(OH)4-]. Therefore, the ionized borate species readily diffuse through the AEM owing to their negative charge.

Even though having a promising potential in terms of energy self-sufficiency, MDCs may suffer from several setbacks such as salinity increase in anolyte having adverse effects on microbial activity, presence of divalent ions in the desalination chamber causing membrane scaling, and membrane fouling. Tackling these challenges will significantly contribute to bringing MDC technology a few steps closer to full-scale applications. Several studies reported the effects of operating parameters on energy production and desalination performance of MDC (Sevda et al., 2017; Ebrahimi et al., 2018; Malakootian et al., 2018). However, most of these studies focused on effect of initial salt concentration, catholyte solution, electrode type, temperature of anolyte solution, and operating time, and there is no study about effect of electrode surface area, air flow rate in cathode chamber, and operating mode on MDC performance. So far, boron removal with MDC has only been studied using synthetic solutions (Ping et al., 2015, 2016). Furthermore, a very recent study by Rahman et al. (2021) has listed several possible modifications to MDC configurations in order to increase system's performance such as flow direction in desalination chamber, membrane spacing, volume, membrane material, electrode material/size, and mode of operation.

In this study, we investigated the performance of MDC in removing boron from synthetic solutions and real geothermal water and in removing COD from yeast industry wastewater, all the while producing energy. Objectives of this study were investigating (i) the effect of electrode surface area, air flow rate, and operating mode on MDC desalination performance, (ii) effect of operational parameters on energy production of MDC and (iii) performance of the optimized system in removal of boron from real geothermal water. It should be noted that this is the first study investigating the effect of electrode area and presenting performance of MDC on boron removal from real geothermal water. Consequently, this study is the most comprehensive study on applicability of a lab-scale MDC for simultaneous wastewater treatment, boron removal and energy production at optimum operating conditions.

2. Materials and methods

2.1. MDC set up and operation

A specifically designed MDC bioreactor consisted of rectangular prism plexiglass chambers: anode, desalination, and cathode chambers (Fig. 1). The dimensions of each identical chamber was 15 cm × 6 cm × 6 cm. Anode/desalination chambers and desalination/cathode chambers were separated using an anion exchange membrane (AEM, AMI-7001, Membrane International Inc., USA) and a cation exchange membrane (CEM, CMI-7000, Membrane International Inc., USA), respectively. Chambers were clamped together with gaskets and O-rings using stainless steel bolts. Carbon graphite sheets of varying areas (18–72 cm^2) were used as electrodes, which were connected by a copper wire completing the electrical circuit.

Anaerobic activated sludge from the wastewater treatment plant of a food-grade yeast production facility was used as seed in the anode chamber. Also, wastewater taken from primary clarification tank of the same treatment plant was used as the source of organic substrate. Chemical Oxygen Demand (COD) and Total Kjeldahl Nitrogen (TKN) values for the yeast wastewater (pH 7.91) were 9280 mg L^{-1} and 413.75 mg L^{-1}, respectively. Anode chamber was filled with a mixture of activated sludge (270 mL) and yeast wastewater (270 mL) for all experiments. Synthetic boron solutions (5, 10 and 20 mg L^{-1}) and real geothermal water were fed to desalination chamber at different runs. During operation, anode chamber and desalination cell were put on a magnetic stirrer with temperature control. Continuous stirring was applied in anode chamber in order to prevent sludge settling. Also temperature was adjusted to maintain 40 °C in desalination chamber, simulating field conditions for a future scale-up. The B solutions were prepared using boric acid (H_3BO_3, Sigma-Aldrich), and solution pH was adjusted to 9.5 using 0.1 M sodium hydroxide (NaOH, Merck-Millipore). The real geothermal water was obtained from Balçova Geothermal Power Plant in İzmir, Turkey. The pH and electrical conductivity of geothermal water were 8.04 and 1770 μS cm^{-1}, respectively. Physicochemical properties of yeast wastewater and real geothermal water were listed in Table S1. Phosphate buffer (0.1 M, pH 6.5), acidified water (pH 2.5) and regular tap water (pH 7.1) were used as catholytes. Various aeration rates (0, 1 and 2 L min^{-1}) were also investigated at the cathode chamber. Samples for analyses were collected from each chamber at specified time intervals. All experiments were conducted in batch mode at 40 °C and operating time of 12 d. Experimental runs were summarized in Table 1.

Most of the experimental runs were conducted in the batch mode (R1-R11). We started the experimental run once by filling the anode, cathode and desalination chambers with their respective solutions and operating the MDC until approximately 90% of the organic substrate in

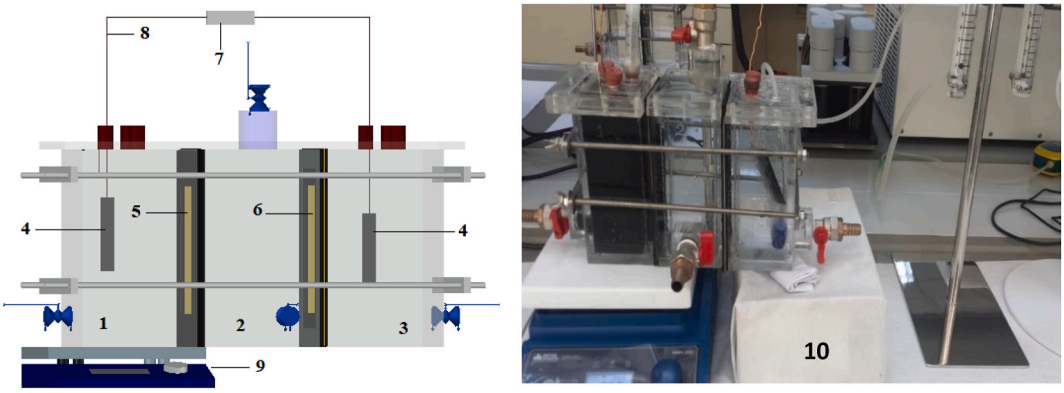

Fig. 1. Schematic diagram of MDC bioreactor: (1) Anode chamber, (2) Desalination chamber, (3) Cathode chamber, (4) Carbon graphite electrode, (5) AEM, (6) CEM, (7) External resistor, (8) Copper wire, (9) Mechanic stirrer, (10) Lab-scale MDC.

Table 1
Experimental runs with different operating parameters. SS: synthetic solution, RGW: real geothermal water.

Experimental Run (R)	Operation Mode	Desalination Chamber	Initial B Concentration (mg L^{-1})	Electrode Surface Area (cm^2)	Catholyte Aeration (L min^{-1})	Catholyte Type
1	Batch	SS	5	36	0	PBS
2			10			
3			20			
4			5		1	
5					2	
6				18		
7				24		
8				72		
9				36		Acidified Water
10						Tap Water
11		RGW	10.5			PBS
12	Fed-Batch	SS	5			
13			10			
14			20			

anolyte – measured by COD – was depleted, which corresponded to 12 d of operation. In the fed-batch mode, at the end of 12 d, we drew treated wastewater from the anode chamber and fed fresh wastewater in the same volume we drew.

2.2. Analytical methods and calculations

Voltage (V) in the open circuit of MDC was continuously recorded every 15 min using a data logger (UNI-T, UT71C Digital Multimeter, China) by connecting to the computer. During operation, pH was measured daily by a pH meter (Mettler Toledo, SevenCompact™, Switzerland). COD was measured through the closed reflux titrimetric method (APHA, 2017). Power density was calculated based on water desalination. An inductively coupled plasma atomic emission spectrometer (ICP-AES, AGILENT 5110, USA) was used to determine the boron concentration at specified operating times. AEM surfaces (facing both the anode and desalination chamber), CEM surfaces (facing both the cathode and desalination chamber), and carbon graphite electrodes were investigated using scanning electron microscopy (SEM, Quanta 250FEG, USA). Energy dispersive X-ray spectrometry (EDX) was also performed for analyzing main elements present on the AEM and CEM surfaces. All analyses were conducted with triplicate measurements and average data were reported. Standard deviation values were calculated to be between 0.01 and 0.015 mg L^{-1}.

The current (I) through the electrical circuit was determined from the measured voltage under 100 Ω external resistance (R_{ex}) according to the following equation:

$$V = IR_{ex} \tag{4}$$

Power density (P, mW m^3) was calculated per volume (v, m^3) of anode chamber using the following equation:

$$P = VI/v \tag{5}$$

Furthermore, the coulombic efficiency (CE, %) for decomposition of organic matter was calculated by following equation (6):

$$CE(\%) = \frac{MW_{O2}\int_0^t Idt}{nFV_a\left(C_{COD,i} - C_{COD,e}\right)} * 100 \tag{6}$$

where MW_{O2} is the molecular weight of oxygen (32 g mol^{-1}), n is number of the e^- transferred from organic matter degradation (n: 4 mol^- mol^{-1}), F is the Faraday's constant (96,485C mol^{-1}), $C_{COD,i}$ is the total input COD concentration in anode chamber (9.228 g L^{-1}), $C_{COD,e}$ is the effluent COD concentration in anode chamber, and V_a is the volume of anode chamber (0.54 L).

3. Results and discussion

3.1. Synthetic solution experiments: energy production, removal of boron and COD

MDC performance may be affected by various operating parameters such as catholyte and anolyte solutions, electrode and membrane materials, size and number of chambers, organic and salt content of wastewater, temperature, and concentration of saline water (Al-Mamun et al., 2018). These operating parameters determine wastewater treatment efficiency, desalination efficiency, COD removal, and energy production. In this study, effects of initial boron concentration, air flow

rate, electrode surface area, and operating mode of the system were investigated to enhance the energy production, and removal efficiencies for boron and COD (Table 1).

A negative control experiment was performed under the optimum operating conditions (initial boron concentration of 5 mg L^{-1}, electrode surface area of 36 cm^2, catholyte solution of PBS buffer, and air flow rate of 2 L min^{-1}) without bacteria to determine the difference, if any, in boron removal efficiency during the same period of time as the biotic experiments. It was clearly seen that in the absence of microbial population only a small fraction of boron content (1.31 mg L^{-1}) was removed from the desalination chamber, most probably being accumulated on the AEM, and rate of diffusion was significantly impaired due to lack of electrochemical gradient.

3.1.1. Effect of initial boron concentration

Initially, MDC was operated using different initial boron concentrations of 5 mg L^{-1} (R1), 10 mg L^{-1} (R2) and 20 mg L^{-1} (R3) at specified operating parameters (Table 1). The maximum boron removal efficiencies were 39.7% ($C_{f,B}$: 12.07 mg L^{-1}), 39.4% ($C_{f,B}$: 6.06 mg L^{-1}) and 45.2% ($C_{f,B}$: 2.74 mg L^{-1}) for R3, R2, and R1, respectively (Fig. 2a, c, 2e). Residual boron concentrations for all runs not only exceeded the WHO limit value for agricultural irrigation (1 mg L^{-1}), but they also exceeded 2.4 mg L^{-1}, which was the limit value for safe drinking water according to WHO guidelines (WHO, 2011).

Energy production and ion concentration gradient were reported as the two main driving forces for salt removal in MDC systems which accelerate desalination at higher salt concentrations (Yang et al., 2015). On the other hand, Ping et al. (2015) studied B removal from aqueous solutions using MDC-Donnan dialysis hybrid system and they reported increased efficiency with decreasing salt loading rate. Similar to the results obtained in the literature, we found that the B removal efficiency seemed to increase with decreasing initial concentration. It should also be noted that the removed portion of the boron concentration in R1 and R3 were 2.26 mg L^{-1} and 7.93 mg L^{-1}, respectively. When the ion concentration difference between the desalination chamber and anode chamber was high, as it was the case in R3, even though more boron was removed from the desalination chamber comparative to R1, the removal efficiency was calculated to be 39.7%, which was lower than the efficiency calculated for R1, 45.2%. Consequently, in our opinion, using absolute measures instead of relative ones was more straightforward in the reporting of initial boron concentration related experimental data. High ion transfer to the electrochemical cells could contribute to charge accumulation and extended desalination times at higher salt concentrations. Therefore, B removal efficiency could be improved with increasing operating time with fed-batch mode.

In addition, B concentrations in anode chamber were measured to investigate a possible boron toxicity on anaerobic microorganisms. At the end of 12 d, boron concentrations in anolyte were 1.42 mg L^{-1}, 1.77 mg L^{-1}, and 5.92 mg L^{-1} for R1, R2, and R3, respectively. The remaining boron in the desalination solution dropped from 20 to 12.07 mg L^{-1}, and the boron content in anolyte solution increased from 0 to 5.92 mg L^{-1} and the remaining boron was detected on the membrane surface. Similar results were observed for the initial boron concentrations of 5 and 10 mg L^{-1}. None of the B concentrations observed in anolyte had a significant adverse effect on COD removal (Fig. 2b, d, 2f). Therefore, based on the COD removal efficiencies it could be concluded that boron had no toxic effect on microorganisms. The COD concentration decreased from 9200 to 415 mg L^{-1} at R3 at the end of the 12 d operation, resulting in a 95.5% removal efficiency. For R1 and R2, removal efficiencies were 89.4% (C_{COD}: 978.9 mg L^{-1}) and 90.0% (C_{COD}: 918.2 mg L^{-1}), respectively. Initial boron concentrations did not seem to have a significant effect on COD removal efficiency.

Daily pH measurements in chambers showed decrease from 9.5 to 8.38 after 1 d of operation at desalination chamber using PBS buffer as the catholyte solution (Fig. S1a). Adjustments to pH 9.5 using NaOH solution (0.1 N) were done daily. Boron transforms to borate ions with larger hydrated radius and negative charge at pH values above 9.14 (Kabay and Bryjak et al., 2015). Thus, raising pH above the pK_a value of 9.14 in desalination chamber was critical in order to sustain removal of boron at MDC. On the other hand, no significant changes in pH at anode and cathode chambers were observed.

The maximum open circuit voltage (OCV) values were measured to be 852 mV (20 mg L^{-1} B), 783 mV (10 mg/L B) and 669 mV (5 mg L^{-1} B) (Fig. S2a). The voltage was almost stable at maximum voltage for 2 d which indicated that the microorganisms were successfully grow and produced enough electron for the energy production at the anode chamber. Furthermore, to understand the power density, the anode and cathode chambers connected with external resistance of 100 Ω. The results showed that the power density increased with time and attained maximum power density of 13.44 mW m^{-3} in 10 d for initial boron concentration of 20 mg L^{-1}. We observed that OCV increased with increasing initial boron concentration. When increasing initial boron concentration, because of a stronger driving force owing to increasing ionic strength of the water, the OCV was improved to a higher level. The maximum power density values were calculated to be 13.44 mW m^{-3} (20 mg L^{-1} B), 11.35 mW m^{-3} (10 mg L^{-1}B), and 8.29 mW m^{-3} (5 mg L^{-1} B) (Fig. S2b). A sudden surge in cell voltage was measured at day 1 due to the fresh source of electron donors (anaerobically acclimatized yeast wastewater), producing values of 760, 620, and 610 mV at 20, 10, and 5 mg L^{-1} B, respectively. After the cell voltages increased to reach previously mentioned maximum values, they entered a slightly decreasing trend most probably due to increase in internal resistance, which was the result of conductivity reduction and substrate depletion in anode chamber.

The overall CE was a function of COD concentration in anode chamber. CE values were determined by integrating the measured current relative to the theoretical current based on the consumed organic matter in anode chamber. The CE values were 12.6–15.3% across a range of initial boron concentration from 5 to 20 mg L^{-1}. The highest CE value was 15.3% at initial boron concentration of 20 mg L^{-1}. The higher CE value obtained at initial boron concentration of 20 mg L^{-1}could be attributed to higher concentration gradient lowering over potential caused by mass transport limitation on the anode electrode surface and anion exchange membrane surface. The CE values observed in this study were comparable with the other studies using synthetic wastewater as substrate. Anusha et al. (2018) studied on application of silver-tin dioxide composite cathode catalyst for enhancing performance of microbial desalination cell and the highest coulombic efficiency was found to be 14.4 ± 0.2% in a five-chambered MDC. In a separate study, the methylene blue removal using polypyrrole modified cathode in bio-electro Fenton coupled with MDC was studied and the average CE was found as 28.8% (Huang et al., 2018).

3.1.2. Effect of airflow rate

Effect of varying aeration rates on the removal of boron were investigated at specified air flow rates of 0 L min^{-1} (R1), 1 L min^{-1} (R4) and 2 L min^{-1} (R5) (Fig. 3). Initial boron concentration was 5 mg L^{-1} and other operating parameters were kept constant (Catholyte solution: PBS buffer, $S_{electrode}$: 36 cm^2).

Microorganisms metabolizing the organic substrate at anode chamber produced electrons (e^-) which were transferred via the electrical circuit to the terminal electron acceptor of oxygen at the cathode chamber (Mirzaienia et al., 2016). With increasing dissolved oxygen concentration, boron removal efficiency increased. In the absence of supplied oxygen (no aeration), boron concentration decreased from 5 mg L^{-1} to 2.74 mg L^{-1}. With aeration in the cathode chamber, initial boron concentration of 5 mg L^{-1} was reduced below 2.4 mg L^{-1} meeting the boron limits set by WHO in drinking water. Maximum boron removal efficiencies were 45.2% ($C_{f,B}$: 2.74 mg L^{-1}), 51.5% ($C_{f,B}$: 2.425 mg L^{-1}), and 61.3% ($C_{f,B}$: 1.935 mg L^{-1}) at R1, R4, and R5, respectively. Increasing concentration of dissolved oxygen facilitated the e^- transfer from anode chamber to cathode chamber, thereby consecutively

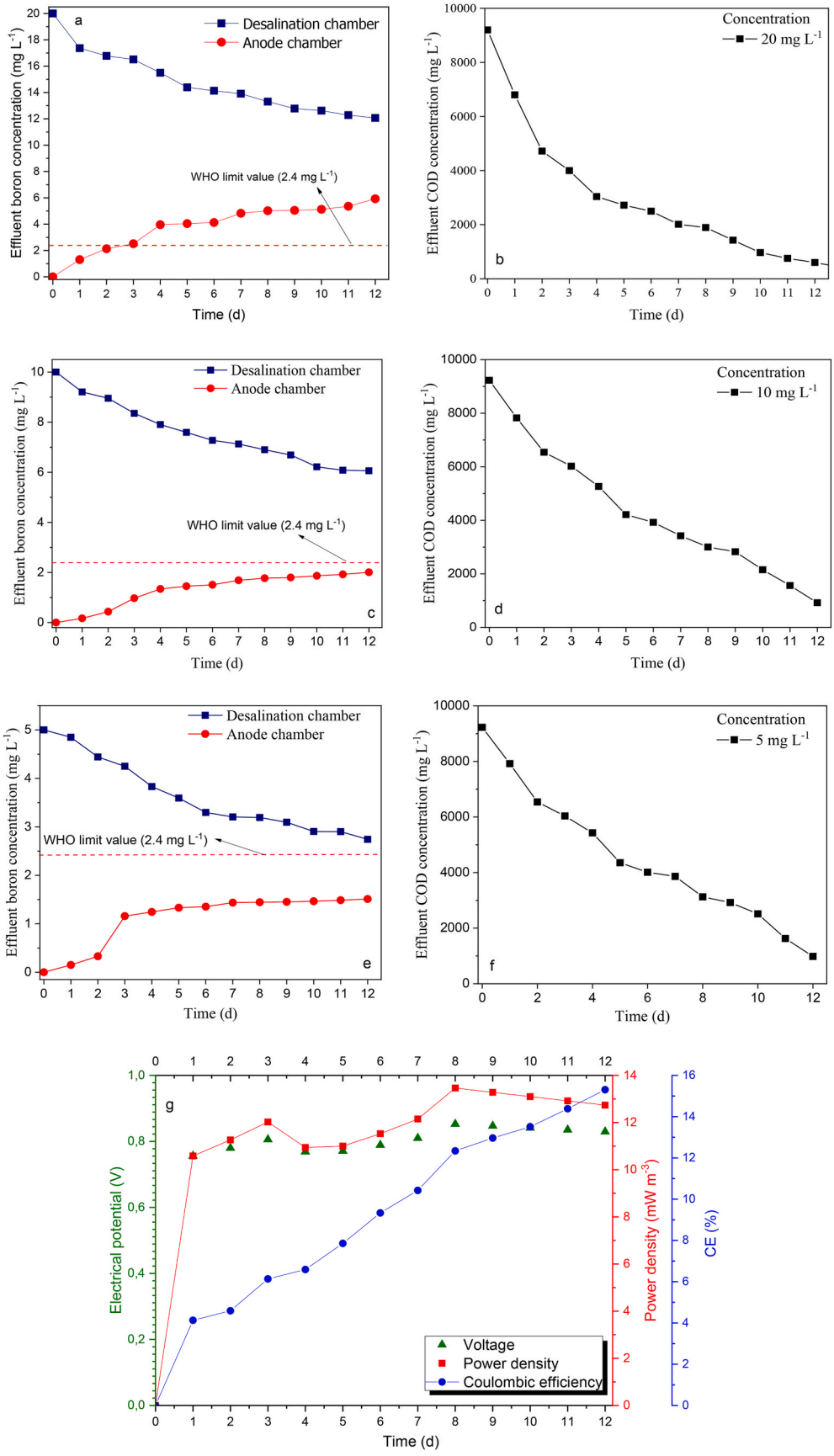

Fig. 2. Effluent boron concentration in the anode and desalination chamber and COD concentration in the anode chamber (a–b) 20 mg L^{-1} boron, (c–d) 10 mg L^{-1} boron, (e–f) 5 mg L^{-1} boron, and (g) electrical potential, power density, and CE at optimum initial boron concentration. (electrode surface area: 36 cm^2, catholyte solution: PBS buffer, and air flow rate: 2 L min^{-1}).

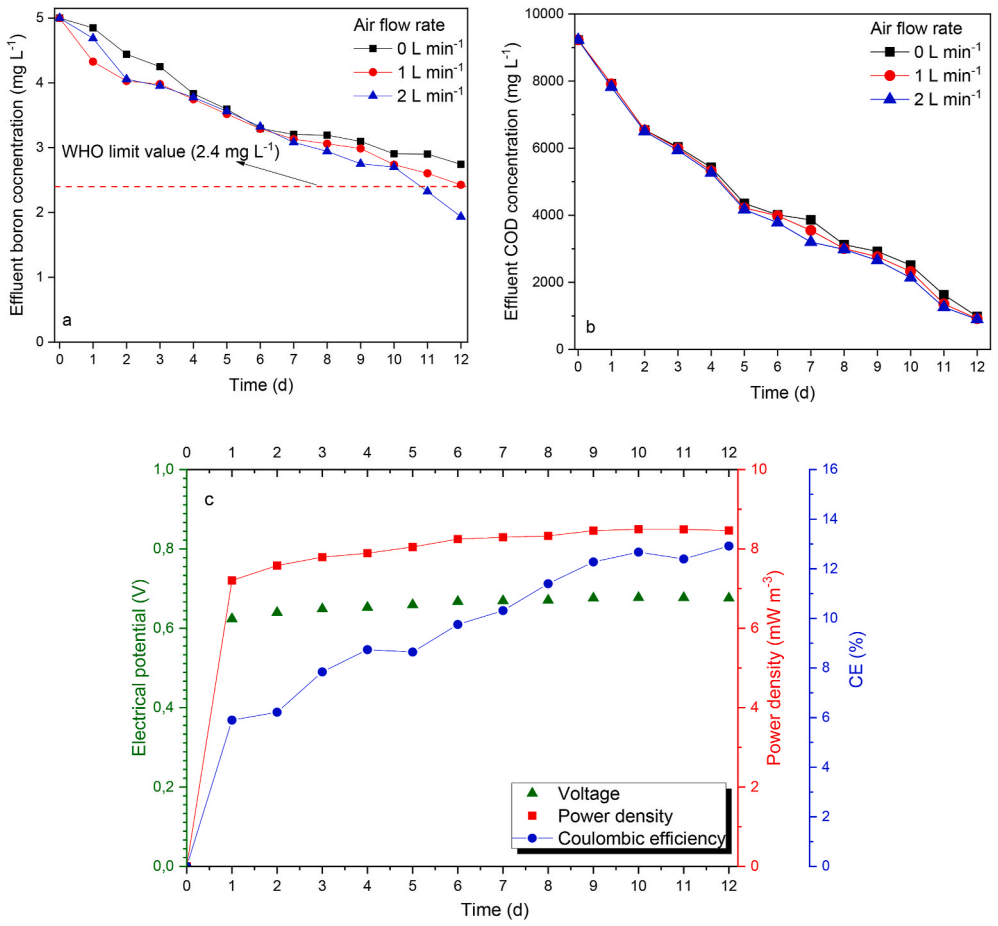

Fig. 3. Effect of air flow rate on effluent boron concentration (a), COD concentration, and electrical potential, power density, and CE at optimum air flow rate (c). (C_{Boron}: 5 mg L^{-1}, electrode surface area: 36 cm^2, catholyte solution: PBS buffer).

improving electrical potential gradient and boron removal efficiency (Bergel et al., 2015). This was also observed in the measured OCV values of the system, which were measured to be 660 mV (R1), 668 mV (R4), and 676 mV (R5) (Fig. S3a-b). Similarly, the power density of the system increased from 7.71 mW m^{-3} (R1) to 8.46 mW m^{-3} (R4). Results showed that the OCV and power density increased with increasing air flow rate in cathode chamber due to the increased e^- acceptor (O_2) concentration in chamber, which caused improved e^- transfer from anode chamber to cathode chamber, resulting in low internal resistance due to increased electrical potential gradient. Consequently, these results demonstrated that air supply was beneficial in terms of enhanced power generation. Rest of the experimental runs were conducted with 2 L min^{-1} aeration.

The CE values were also found to be 12.7, 12.8, and 12.9% for air flow rate of 0, 1, and 2 L min^{-1}, respectively. The cathode chamber was aerated with the O_2 which dramatically facilitated the electron transfer, it could be reasonable to expect a decrease in the MDC internal resistance. The decreased in internal resistance most probably reduce the MDC energy loss during electron transfer and thus enhance the CE. These results are good agreement with the literature. The removal of ammonium and phosphate ions using MDC with carbon cloth as air cathode and the CE values of the system were in the range of the 7–15% (Chen et al., 2015). In a separate research, electricity production and desalination in a separator coupled stacked microbial desalination cell with buffer free electrolyte circulation was studied. The CE values were determined for three types of reactors and the CE values were reported in the range of 11–64% (Chen et al., 2012). Overall, our results demonstrated that air supply is beneficial in terms of high cell potential, power production, CE.

Malakootian et al. (2018) studied arsenic removal from aqueous solutions using MDC and they found that the arsenic removal efficiency increased with increasing dissolved oxygen concentration. The maximum arsenic removal efficiency was found to be 75.0% at dissolved oxygen concentration of 6 mg L^{-1} within the operating time of 120 min. In a separate study, Clauwert et al. (2007) studied electricity production using an MFC without air supply and they found that the oxygen in cathode chamber was one of the most important operating parameters.

Results showed that aeration of cathode chamber did not have a significant effect on the COD removal efficiency of MDC. COD removal efficiencies were 89.4% ($C_{f,COD}$: 982 mg L^{-1}), 90.1% ($C_{f,COD}$: 916 mg L^{-1}), and 90.3% ($C_{f,COD}$: 897 mg L^{-1}) for air flow rates of 0, 1, and 2 L min^{-1} at operating time of 12 d, respectively. Previous studies on COD removal using MDC set-ups showed satisfactory COD removal efficiencies. For instance, the maximum COD removal from petroleum refinery wastewater using MDC was 70.5% at initial salt concentration of 20 g L^{-1} and using an acidified catholyte solution (Sevda et al., 2017). In a separate study, the highest COD removal rates from industrial wastewater by microbial fuel cell were in the range of 80–90% (Firdous et al., 2018).

3.1.3. *Effect of electrode surface area*

Electrode material and electrode surface area are important parameters which affect the MDC performance in terms of desalination efficiency, energy production, and wastewater treatment (Wang et al., 2013). Carbon felt, carbon brush, activated carbon cloth, carbon cloth, graphite brush embedded in graphite granules, and graphite paper are commonly used electrode materials in MDC set-ups due to their high stability, conductivity, and low cost (Cao et al., 2009; Pant et al., 2010; Ragab et al., 2019). However, none of the published studies investigated

the effect of electrode surface area on MDC performance. In this study, we investigated the effect of different electrode surface areas of 18 cm^2 (R6), 24 cm^2 (R7), 36 cm^2 (R1), and 72 cm^2 (R8) on boron and COD removal efficiencies (Fig. 4). Initial boron concentration of 5 mg L^{-1} was used at optimized conditions.

Electrode surface area has a great impact on colonization of microorganisms, transportation of organic substrate, and formation of biofilm layer by microorganism. The colonization of microorganisms, transportation of organic substrate, and formation of biofilm layer by microorganisms can probably increase with the increment of the electrode surface area. Above mentioned probabilities were verified with experimental results. As expected, the boron removal efficiencies increased with the increasing electrode surface area. Boron removal efficiencies were measured to be 37.7% ($C_{f,B}$: 3.115 mg L^{-1}), 57.6% ($C_{f,B}$: 2.118 mg L^{-1}), 61.3% ($C_{f,B}$: 1.934 mg L^{-1}), 61.4% ($C_{f,B}$: 1.932 mg L^{-1}) for R6, R7, R1, and R8, respectively. A significant increase in boron removal efficiencies were observed when results from R6 were compared with the other runs. Nevertheless, the removal efficiencies for R1 and R8, giving the maximum removal efficiencies, were practically the same. The bacteria that growth on the anode electrode surface oxidize the organic compounds, whereby generated e^- move towards the cathode electrode. Borate ions moved from the desalination chamber to anode chamber, when electricity is generated concurrently. On the other hand, even if the electrode surface area increases, the amount of microorganisms in the anolyte solution and the amount of e^- they can produce is constant. Therefore, by increasing the surface area to a certain point, it is possible to increase the biofilm in the electrode surface area and thus increase the boron removal. However, the increasing electrode surface area could not show significant effect on removal efficiency due to the limited microorganism amount in anolyte solution. An initial approach of using 36 cm^2 electrodes was proven to be sufficient, since doubling the electrode area has not improved the boron removal efficiency. Rest of the experimental runs were conducted using 36 cm^2 electrodes.

Effluent COD concentrations were found to be 991, 954, 897, and 892 mg L^{-1} for electrode surface areas of 18, 24, 36, and 72 cm^2, respectively. As expected, there was no significant change at COD concentration as there was no change at the activated sludge volume and/or industrial wastewater volume in anode chamber. As a conclusion, changing activated sludge volume or wastewater type to improve microbial activity could be an effective method to improve the performance of MDC. However, there is no study about the effect of anaerobic activated sludge volume in anode chamber on MDC removal and energy production efficiency. Moreover, effect of electrode surface areas on OCV and power production were investigated (Fig. S4a-b). The highest OCV and power densities were found to be 607 mV and 6.83 mW m^{-3} (R6), 612 mV and 6.94 mW m^{-3} (R7), 676 mV and 8.46 mW m^{-3} (R1), 678 mV and 8.52 mW m^{-3} (R8), respectively. The higher electrode surface area favored OCV and power density of the system owing to the higher e^- accumulation with the higher microorganism colonization on electrode surface area. These results confirmed that the electrode surface area can be significant operating parameter of MDC system.

As expected, the CE values increased with increasing electrode surface area from 18 to 72 cm^2. However, there was no significant difference in terms of CE values between 18 and 24 cm^2 and 36–72 cm^2 electrode surface experiments. The CE values were found to be 11.7, 11.8, 12.9, and 13.0% for electrode surface areas of 18, 24, 36, and 72 cm^2, respectively. Highest CE values were achieved at both electrode surface areas of the 36 and 72 cm^2 owing to decrease in internal resistance with the increasing biofilm formation resulted with high electron production and organic matter degradation.

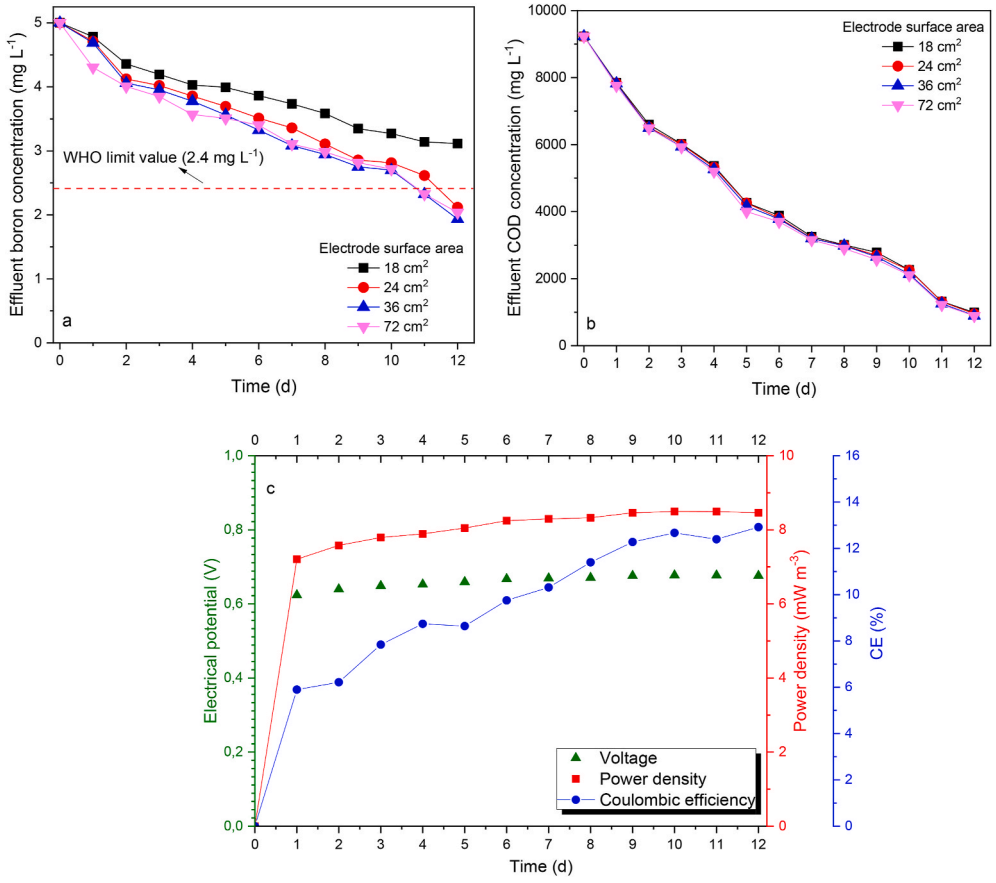

Fig. 4. Effect of electrode surface area on effluent boron concentration (a), COD concentration (b), and electrical potential, power density, and CE at optimum electrode surface area (c). (Catholyte solution: PBS buffer, C_{Boron}: 5 mg L^{-1}, air flow rate: 2 L min^{-1}).

3.1.4. Effect of catholyte solution

Phosphate buffer, ferricyanide, sodium acetate, and sodium chloride solutions, sodium phosphate buffer brackish water, mineral solution with microalgae as biocatalyst, and acidified water were commonly used as the catholyte solution in MDCs (Cao et al., 2009; Kim and Logan, 2011; Jacobsan et al., 2011a, 2011b; Morel et al., 2012; Qu et al., 2012; Davis et al., 2013; Ge et al., 2014; Wen et al., 2014). There is a requirement for a cost effective, environmentally safe, and efficient catholyte solution for possible commercialization and scale-up of MDCs. Therefore, it is important to find the most suitable catholyte solution in order to develop cost effective and commercially feasible MDCs for boron removal from aqueous solutions. In this study, phosphate buffer (R1), acidified water (R9) and regular tap water (R10) were investigated as catholyte solutions (Fig. 5).

Results showed that boron removal efficiency decreased when acidified water and tap water were used as catholyte solution. At the end of the operating time of 12 d, boron removal efficiencies were found to be 61.32% ($C_{f,B}$: 1.934 mg L^{-1}), 44.1% ($C_{f,B}$: 2.795 mg L^{-1}), and 40.3% ($C_{f,B}$: 2.986 mg L^{-1}) for R1, R9 and R10, respectively. It should be considered that the concentration gradient of catholytes in MDC system might increase water flux from cathode chamber to desalination chamber. In MDC using PBS solution, the borate ion transfer was more efficient than that obtained through acidified water and tap water solution which led to a high performance of non-buffer saline catholyte in spite of pH imbalance. Furthermore, the boric acid was most probably remaining uncharged form due to the significant pH imbalance in desalination solution using acidified and tap water, which inhibit the formation of negatively charged borate ions and so effective removal of boron. When low concentration of phosphate buffer was used, the ions concentration in desalination chamber could become higher than that of the cathode chamber. Therefore, water would move from cathode chamber to desalination chamber because of salt gradient, which might lead to higher desalination rate in MDC. However, Kim and Logan (2013) stated that these effects were negligible.

High concentrations of oxygen present in cathode chamber improved OH^- release, facilitating greater migration of positively charged ions from desalination chamber to cathode chamber. The close boron removal rate achieved in this study could be explained by the ionic charge of boron. As boron was negatively charged in desalination chamber, no significant effect of catholyte solution on boron removal was observed.

pH changes in desalination and cathode chamber were observed during operation (Fig. S1b). Acidified water solution resulted in the highest pH variation in desalination chamber, decreasing from 10.5 to 6.54 during the first 24 h of operation. The main reason that acid solution reduced boron removal efficiency could be explained by desalination solution becoming acidic, resulting in boron remaining in the form of uncharged boric acid. Cathode chamber's pH exhibited the quite opposite trend with an increase from 2.5 to 5.78 in the first 24 h. The anolyte solution showed the lowest pH variation when acidified water

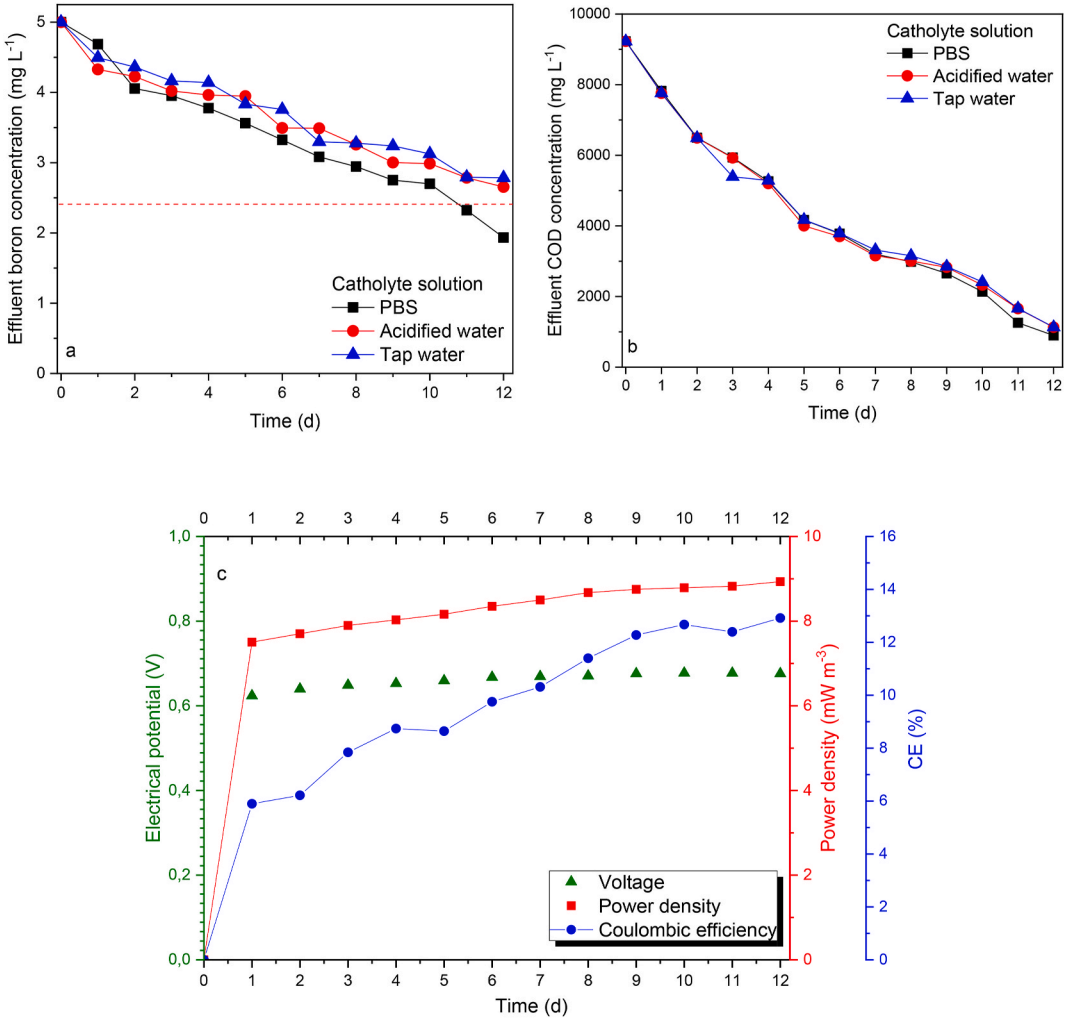

Fig. 5. Effect of catholyte solution on effluent boron concentration (a), COD concentration (b), and electrical potential, power density, and CE at optimum catholyte solution (c). (C_{Boron}: 5 mg L^{-1}, electrode surface area: 36 cm^2, and air flow rate: 2 L min^{-1}).

used as catholyte solution. On the other hand, MDC using phosphate buffer and tap water showed relatively lowest pH variation at desalination solution. The pH in desalination chamber decreased from 10.5 to 8.97 and 10.5 to 8.53 during the first 24 h of the operation for PBS buffer and tap water, respectively. No significant pH change was observed in anolyte for phosphate buffer and tap water solutions. Furthermore, effluent COD concentrations were found to be 897, 1128, and 1132 mg L^{-1} for R1, R9, and R10, respectively. As expected, there was no significant change at COD concentration.

The maximum OCV and power density values at R10, R1, and R9 were 642 mV and 7.61 mW m^{-3}, 676 mV and 8.93 mW m^{-3}, 714 mV and 9.43 mW m^{-3}, respectively (Fig. S5a-b). The lowest power density and OCV was achieved using tap water due to the low cell potential related to neutral pH of the solution. In contrast with tap water and PBS buffer, obtained results indicated that the acidified water increased OCV and power density of MDC due to the higher cell potential owing to lower pH of the solution. Furthermore, the acidified water caused significant pH variations in MDC system, which is resulted with excess chemical consumption due to the need of pH adjustment. Since the best results were obtained with PBS as catholyte, it was used for the rest of the experiments.

Furthermore, the effects of different catholyte solutions on CE values were determined and the maximum CE values were found to be 12.6, 12.9, and 14.0% for tap water, PBS buffer, and acidifiec water, respectively. These results obviously showed that the highest CE values were achieved at acidified water showing that the combination of oxygen and wastewater as the electron acceptor had the considerable benefit in CE. Since it is a strong oxidant and quickly depletes all the electrons in the cathode chamber and exerts a strong pull on electrons from the anode, as well as having good buffer capacity (Pandit et al., 2011).

3.1.5. Fed-batch operating mode

The effect of fed-batch operating mode on boron and COD removal was also investigated for varying initial boron concentrations (5 mg L^{-1} – R12, 10 mg L^{-1} – R13 and 20 mg L^{-1} – R14) at three cycles under determined optimum operating conditions (Fig. S6). Treated industrial wastewater in anode chamber was removed from the cell at the end of the operating time of 12 d (1st cycle), then fresh industrial wastewater was fed in anode chamber and it was repeated twice. Results showed continued decrease in boron concentrations under fed-batch operating mode. Effluent boron concentrations were 1.93, 1.46, and 1.05 mg $L^{-1}$for initial boron concentration of 5 mg L^{-1} at the end of cycles 1, 2, and 3, respectively. The highest boron removal efficiency was found to be 79% at the end of the third cycle. At the end of 12 d operations, boron migration from desalination chamber to anode chamber was quite slow as the system reached saturation. However, migration of B from desalination chamber to anode chamber was facilitated with the feed of fresh wastewater in anode chamber due to the increasing concentration gradient. The highest boron removal efficiencies were also found to be 78.8 and 74.5% for initial boron concentrations of 10 and 20 mg L^{-1} at the end of the third cycle, respectively. Furthermore, COD removal efficiencies were 89.7, 90.2, and 95.6% for R14, R13 and R12 at the end of each cycle. Results showed that there was no significant change in COD removal efficiency values at all cycles for different boron concentrations.

Results concluded that the boron removal efficiency of the MDC system was enhanced with fed-batch operation mode. Luo et al. (2012) studied desalination, wastewater treatment, and energy production using MDC in fed-batch mode. They reported that the maximum salt removal efficiency, COD removal efficiency and power production were 66.0%, 53.8% and 8 W m^{-3} at optimum operating conditions in fed-batch mode. In a separate study, the highest power production and salt removal efficiency were found to be 1.1 W m^{-3} and 64.2% using micro-algae and synthetic wastewater as a catholyte and anolyte solution, respectively (Kokabian et al., 2015). These studies showed that results were good agreement with the literature. Moreover, the COD and desalination efficiency of proposed MDC system were significantly high compared to the literature.

3.2. Membrane fouling and biofilm formation in MDC

SEM images of AEM and CEM before (Fig. 6a and d) and after (Fig. 6b, c, 6e, 6f) the experimental runs were investigated. AEM images implied that the anode side of the AEM was colonized by microbes, forming a biofilm layer on membrane surface (Fig. 6b). On the other hand, the desalination chamber side of the AEM did not show any signs for agglomeration of microbial origin but that of coarser grains (Fig. 6c). In addition, the CEM surfaces facing desalination chamber and catholyte solution were covered with coarser crystal shape aggregations (Fig. 6e and f). Biofilm formation on membrane surface might cause a decrease in membrane resistance, deterioration of membrane structure, and decrease of ion transfer and flux through membranes.

The EDX results also showed a change of ion content on the membrane surfaces (Table S2). Carbon content of the AEM surface facing with anode solution decreased considerably from the initial 59.84%–49.38%. The decreasing carbon content and increasing oxygen content was predicted to be on account of the deposition of organic matters on the AEM surface facing anode solution. Elements such as B and Cl were present on AEM surface after the operation. The B content of AEM was found to be 30.25 and 28.21% for surfaces facing anode solution and desalination solution, respectively. The presence of B and Cl elements were due to the transfer of anions from the desalination chamber and the composition of the wastewater (Angelov et al., 2013). As expected no significant change in carbon content was observed on the CEM surfaces. Oxygen content has increased significantly on CEM surface facing the catholyte due to active aeration that has been done.

Consequently, it could be concluded that there was more to be done in developing means to find an efficient way for in-situ membrane cleaning and to produce novel membrane materials which were more resistant to biofouling and ion agglomeration in MDC set-ups.

3.3. Boron removal from real geothermal water

An experimental was (R11) performed using real geothermal water at optimized conditions. Effluent boron and COD concentrations of treated geothermal water using MDC were presented in Fig. S7a and S7b, respectively. Boron concentration decreased from 10.5 mg L^{-1} to 5.8 mg L^{-1} at the end of the 12 d in geothermal water. Observed boron removal efficiency for real geothermal water (44.3%) was higher than that for 10 mg L^{-1} B synthetic solution (39.4%) for the same experimental conditions. This was probably due to the high ionic strength of the geothermal water. Concentration gradient of the system increased with the increasing ionic strength of the aqueous solution. As expected, boron removal efficiency of MDC for geothermal water improved owing to increased concentration gradient. Moreover, the COD removal efficiency was 90.6% at real geothermal water, while the COD removal efficiency was found to be 90.0% at 10 mg L^{-1} boron containing synthetic solution removal experiment. These results showed that there was no significant change at COD removal efficiencies for both synthetic and real geothermal water removal experiments.

3.4. Cost assessment of MDC

This study demonstrated that the MDC could desalinate water with high ionic content, such as boron containing aqueous solution, and more complex waters, such as geothermal brine, and reduce energy consumption. The high energy consumption and treated water price are key factors in the operating cost of the desalination processes. Using the MDC, similar boron removal efficiencies were achieved with the single pass reverse osmosis system. While the MDC is an energetically self-sufficient system, reverse osmosis systems consume almost 2.2 kWh of electricity for treatment of 1 m^3 saline water. Furthermore, the MDC has almost 100% water recovery, while reverse osmosis processes maintain

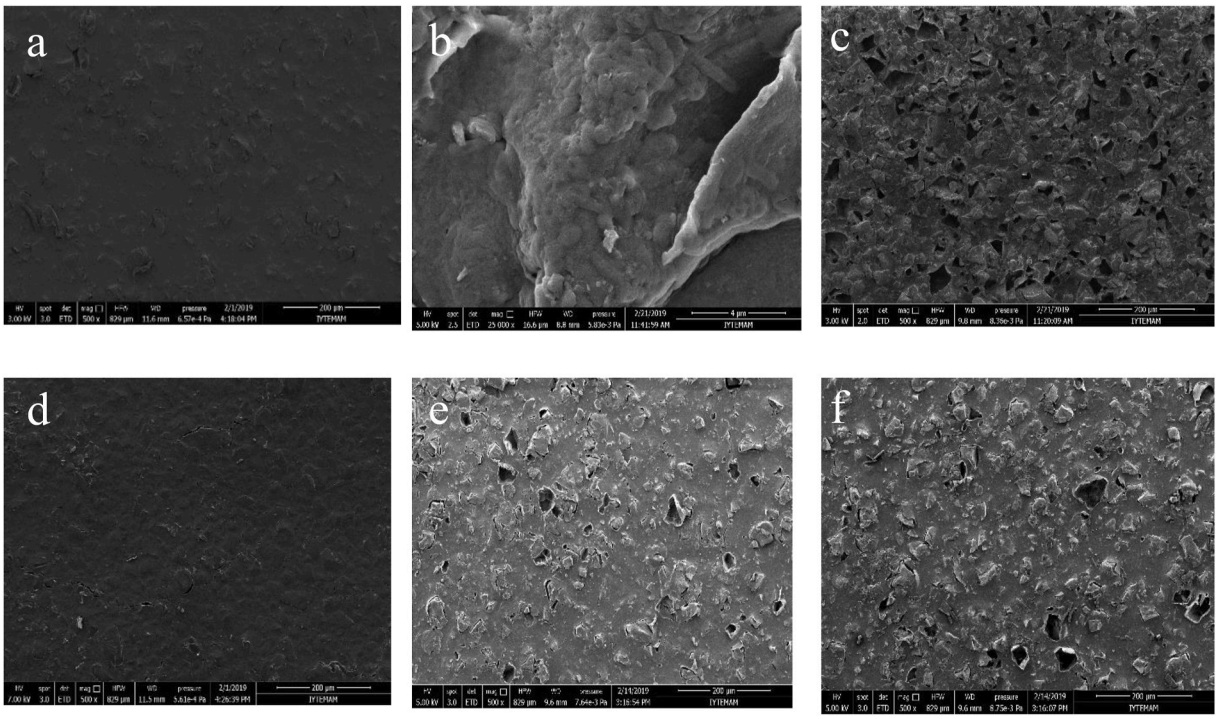

Fig. 6. SEM images of membranes before and after operation. AEM surface before operation(a), AEM surface facing with anode solution (b), AEM surface facing with desalination solution (c), CEM surface before operation (d), CEM surface facing with cathode solution (e), CEM surface facing with desalination solution (f).

about 50% of the feed water as concentrate. In a scenario that conducts the MDC as pre-treatment before conventional desalination processes, the energy required by other desalination processes can be reduced owing to bioenergy production ability of MDC. The energy benefits of MDC processes should be further investigated with pilot scale studies.

A basic cost assessment was carried out to calculate the material cost of the MDC system including, AEM, CEM, carbon electrode, copper wire, Plexiglas, and other apparatus. The total material cost of the system for 540 mL MDC reactor set-up was found to be 30.2 $, and the AEM and CEM accounted for 23.5% of the total material cost. Therefore, the production of cost effective AEM and CEM could significantly reduce the material cost of MDC reactors. Besides, the high capital cost and low water production rates of bio-electrochemical systems are a major problem which hinder the its application in real scale. For instance, to accomplish a similar amount of water production, the MDC needs longer operating time than reverse osmosis processes, which may be balanced using a larger reactor volume, but that in turn increases capital costs. On the other hand, the benefits from wastewater treatment must be considered as MDC processes are an integrated technology of both desalination and wastewater treatment, when evaluating MDCs performance. The MDC systems can be constructed in a location that may access both saline and wastewater streams. Consequently, the capital cost of the MDC system can be similar to that of small scale wastewater treatment plants, with a possibility for further decrease, profiting from the development of low cost ion exchange membrane materials.

3.5. Resource recovery potential of MDC

The studied configuration of MDC allowed for the removed boron from the geothermal brine and synthetic solutions to accumulate at the anode chamber. Since the solution matrix of the anode chamber was quite complex due to activated sludge and yeast industry wastewater, boron recovery was not feasible. However, the primary objective of this study was to desalinate water streams such as geothermal brine that had high ionic content and for this particular study, high boron content. Following desalination, we aimed to produce irrigation quality water since agriculture sector claimed more than 70% of freshwater resources in Aegean region of Turkey, which was also rich in geothermal energy resources. Apart from that, supporting the desalination mechanism with selective adsorbents equipped MDC with the potential for resource recovery from geothermal brine regarding elements such as As, Li and B. Currently, a scaled up hybrid reactor configuration that employs adsorption, electrodialysis and membrane desalination is being studied in our lab.

4. Conclusion

This study revealed MDC as an environmental friendly solution for simultaneous boron removal from geothermal water and COD removal/energy production from industrial wastewater. Among the investigated operating parameters, electrode surface area had the most significant effect on boron removal efficiency, followed by air flow rate and catholyte solution. Furthermore, the removal efficiencies for selected electrode surface areas except for the electrode surface area of 18 cm^2, giving the promising removal efficiencies, were practically the same. Even though the WHO's limit for boron concentrations in drinking waters met the optimized experimental conditions, none of the experiments produced water at irrigation quality. In that aspect, MDC could be used as a polishing step applied to the effluents of other membrane treatment technologies. It was obvious that the factors contributing to the internal resistance such as organic and inorganic membrane fouling and inter-membrane distance had to be tackled in further studies.

Author statement

Aysegul Yagmur Goren: Writing - Original Draft, Methodology, Investigation. **Hatice Eser Okten:** Supervision, Writing - Review & Editing.

Declaration of competing interest

The authors declare that they have no known competing financial

interests or personal relationships that could have appeared to influence the work reported in this paper.

Acknowledgement

Authors would like to thank to Environmental Development, Application and Research Center at IZTECH for boron analyses. Authors would like to thank to Materials Research Center at IZTECH for SEM analyses.

Appendix A. Supplementary data

Supplementary data to this article can be found online at https://doi.org/10.1016/j.chemosphere.2021.131370.

References

Al-Mamun, A., Ahmad, W., Baawain, M.S., Khadem, M., Dhar, B.R., 2018. A review of microbial desalination cell technology: configurations, optimization and applications. J. Clean. Prod. 183, 458–480.
Al-Bsoul, A., Al-Shannag, M., Tawalbeh, M., Al-Taani, A.A., Lafi, W.K., Al-Othman, A., Alsheyab, M., 2020. Optimal conditions for olive mill wastewater treatment using ultrasound and advanced oxidation processes. Sci. Total Environ. 700, 134576.
Al-Qodah, Z., Tawalbeh, M., Al-Shannag, M., Al-Anber, Z., Bani-Melhem, K., 2020. Combined electrocoagulation processes as a novel approach for enhanced pollutants removal: a state-of-the-art review. Sci. Total Environ. 744, 140806.
Angelov, A., Bratkova, S., Loukanov, A., 2013. Microbial fuel cell based on electroactive sulfate reducing biofilm. Energy Convers. Manag. 67, 283–286.
Anusha, G., Noori, Md T., Ghangrekar, M.M., 2018. Application of silver-tin dioxide composite cathode catalyst for enhancing performance of microbial desalination cell. Mater. Sci. Technol. 1, 188–195.
APHA, 2017. Standard Methods for the Examination of Water and Wastewater, Twenty-Three. American Public Health Association Manual, New York.
Arar, Ö., Yüksel, Ü., Kabay, N., Yüksel, M., 2013. Application of electrodeionization (EDI) for removal of boron and silica from reverse osmosis (RO) permeate of geothermal water. Desalination 310, 25–33.
Banasiak, L.J., Schafer, I., 2009. Removal of boron, fluoride and nitrate by electrodialysis in the presence of organic matter. J. Membr. Sci. 334, 101–109.
Barth, S., 2000. Utilization of boron as a critical parameter in water quality for thermal and mineral water resources in SW German and N Switzerland. Environ. Geol. 40, 1–2.
Bergel, A., Feron, D., Mollica, A., 2005. Catalysis of oxygen reduction in PEM fuel cell by seawater biofilm. Electron. Chem. Commun. 7, 900–904.
Bryjak, M., Wolska, J., Kabay, N., 2008. Removal of boron from seawater by adsorption-membrane hybrid process: implementations and challenges. Desalination 223, 57–62.
Cao, X., Huang, X., Liang, P., Xiao, K., Zhou, Y., Zhang, X., Logan, B.E., 2009. A new method for water desalination using microbial desalination cells. Environ. Sci. Technol. 43 (18), 7148–7152.
Chen, X., Liang, P., Wei, Z., Zhang, X., Huang, X., 2012. Sustainable water desalination and electricity generation in a separator coupled stacked microbial desalination cell with buffer free electrolyte circulation. Bioresour. Technol. 119, 88–93.
Chen, X., Sun, D., Zhang, X., Liang, P., Huang, X., 2015. Novel self-driven microbial nutrient recovery cell with simultaneous wastewater purification. Sci. Rep. 5.
Clauwert, P., Van Der Ha, D., Boon, N., Verbeken, K., Verhaege, M., Rabaey, K., Verstraete, W., 2007. Open air biocathode enables effective electricity generation with microbial fuel cells. Environ. Sci. Technol. 41, 7564–7569.
Davis, R.J., Kim, Y., Logan, B., 2013. Increasing desalination by mitigating anolyte pH imbalance using catholyte effluent addition in a multi-anode bench scale microbial desalination cell. Sustaniable Chem. Eng. 1, 1200–1206.
Dominguez-Tagle, C., Romero-Ternero, V.J., Delgado-Tores, A.M., 2011. Boron removal efficiency in small seawater reverses osmosis systems. Desalination 265, 43–48.
Ebrahimi, A., Najafpour, G.D., Kebria, D.Y., 2018. Performance of microbial desalination cell for salt removal and energy generation using different catholyte solutions. Desalination 432, 1–9.
Firdous, S., Jin, W., Shahid, N., Bhatti, Z.A., Iqbal, A., Umara, Abbasi, Mahmood, Q., Ali, A., 2018. The performance of microbial fuel cell streaming vegetable oil industrial wastewater. Environ. Technol. Inno. 10, 143–151.
Ge, Z., Dosoretz, C.G., He, Z., 2014. Effects of number of cell pairs on the performance of microbial desalination cells. Desalination 341, 101–106.
Gude, V.G., 2016. Geothermal source potential for water desalination–current status and future perspective. Renew. Sustain. Energy Rev. 57, 1038–1065.
Hilal, N., Kim, G.J., Somerfield, C., 2011. Boron removal from saline water: a comprehensive review. Desalination 273, 23–35.
Huang, G., Wang, H., Zhao, H., Wu, P., Yan, Q., 2018. Application of polypyrrole modified cathode in bio-electro-Fenton coupled with microbial desalination cell (MDC) for enhanced degradation of methylene blue. J. Power Sources 400, 350–359.
Jacobson, K.S., Drew, D.M., He, Z., 2011a. Efficient salt removal in a continuously operated upflow microbial desalination cell with an air cathode. Bioresour. Technol. 102, 376–380.
Jacobson, K.S., Drew, D.M., He, Z., 2011b. Use of a liter-scale microbial desalination cell as a platform to study bioelectrochemical desalination with salt solution or artificial seawater. Environ. Sci. Technol. 45, 4652–4657.
Kabay, N., Bryjak, M., 2015. Boron Separation Processes. Elsevier, Amsterdam, pp. 219–235.
Kartikaningsih, D., Shih, Y.J., Huang, Y.H., 2016. Boron removal from boric acid wastewater by electrocoagulation using aluminum as sacrificial anode. Sustain. Environ. Res. 1–6.
Kim, Y., Logan, B.E., 2011. Series assembly of microbial desalination cells containing stacked electrodialysis cells for partial or complete seawater desalination. Environ. Sci. Technol. 45, 5840–5845.
Kim, Y., Logan, B.E., 2013. Microbial desalination cell for energy production and desalination. Desalination 308, 122–130.
Kokabian, B., Gude, V.G., 2015. Sustainable photosynthetic biocathode in microbial desalination cells. Chem. Eng. J. 262, 985-965.
Logan, B.E., Cheng, S., Watson, V., Estadt, G., 2007. Graphite fiber brush anodes for increased power production in air-cathode microbial fuel cells. Environ. Sci. Technol. 41, 3341–3346.
Luo, H., Xu, P., Roane, T.M., Jenkins, P.E., Ren, Z., 2012. Microbial desalination cells for improved performance in wastewater treatment, electricity production, and desalination. Bioresour. Technol. 105, 60–66.
Malakootian, M., Mirzaienia, F., Malakootian, M., 2018. Investigation of the efficiency of microbial desalination cell in removal of arsenic from aqueous solutions. Desalination 438 (15 July 2018), 19–23.
Mirzaienia, F., Asadipour, A., Jafari, A.J., Malakootian, M., 2016. Removal efficiency of nickel and lead from industrial wastewater using microbial desalination cell. Appl. Water Sci. 1–8.
Morel, A., Zuo, K., Xia, X., Wei, J., Luo, X., Liang, P., Huang, X., 2012. Microbial desalination cells packed with ion-exchange resin to enhance water desalination rate. Bioresour. Technol. 118, 43–48.
Nielsen, F.H., 2002. The Nutritional Importance and Pharmacological Potential of Boron for Higher Animals and Human. Springer, pp. 37–49.
Ozbey-Unal, B., Imer, D.Y., Keskinler, B., Koyuncu, I., 2018. Boron removal from geothermal water by air gap membrane distillation. Desalination 433, 141–150.
Pandit, S., Sengupta, A., Kale, S., Das, D., 2011. Performance of electron acceptors in catholyte of a two-chambered microbial fuel cell using anion exchange membrane. Bioresour. Technol. 102, 2736–2744.
Pant, D., Van Bogaert, G., Diels, L., Vanbroekhoven, K., 2010. A review of the substrates used in microbial fuel cells (MFCs) for sustainable energy production. Bioresour. Technol. 101, 1533–1543.
Ping, Q., Abu-Ressh, I.M., He, Z., 2015. Boron removal from saline water by a microbial desalination cell integrated with donnan dialysis. Desalination 376, 55–61.
Ping, Q., Abu-Ressh, I.M., He, Z., 2016. Mathematical modeling based evaluation and simulation of boron removal in bioelectrochemical systems. Sci. Total Environ. 569–570, 1380–1389.
Qu, Y., Feng, Y., Wang, X., Liu, J., Lv, J., He, W., Logan, B.E., 2012. Simultaneous water desalination and electricity generation in a microbial desalination cell with electrolyte recirculation for pH control. Bioresour. Technol. 106, 89–94.
Ragab, M., Elawwad, A., Abdel-Halim, H., 2019. Simultaneous power generation and pollutant removals using microbial desalination cell at variable operation modes. Renew. Energy 143, 939–949.
Rahman, S., Jafary, T., Al-Mamun, A., Baawain, M.S., Choudhury, M.R., Alhaimali, H., Siddiqi, S.A., Dhar, B.R., Ranjan, B., Sana, A., Lam, S.S., Aghbashlo, M., Tabatabaei, M., 2021. Towards upscaling microbial desalination cell technology: a comprehensive review on current challenges and future prospects. J. Clean. Prod. 288, 125597.
Recepoğlu, Y.K., Kabay, N., Ipek, I.Y., Arda, M., Yüksel, M., Yoshizuka, K., Nishihama, S., 2018. Packed bed column dynamic study for boron removal from geothermal brine by a chelating fiber and breakthrough curve analysis by using mathematical models. Desalination 437, 1–6.
Ren, L., Ahn, Y., Hou, H., Zhang, F., Logan, B.E., 2014. Electrochemical study of multi-electrode microbial fuel cells under fed-batch and continuous flow conditions. J. Power Sources 257, 454–460.
Sevda, S., Abu-Reesh, I.M., Yuan, H., He, Z., 2017. Bioelectricity generation from treatment of petroleum refinery wastewater with simultaneous seawater desalination in microbial desalination cells. Energy Convers. Manag. 141, 101–107.
Tawalbeh, M., Al-Othman, A., Singh, K., Douba, I., Kabakebji, D., Alkasrawi, M., 2020. Microbial desalination cells for water purification and power generation: a critical review. Energy 209, 118493.
Wang, H., Wang, G., Ling, Y., Qian, F., Song, Y., Lu, X., Chen, S., Tong, Y., Li, Y., 2013. High power density microbial fuel cell with flexible 3D graphene–nickel foam as anode. Nanoscale 5, 10283–10290.
Wen, Q., Zhang, H., Yang, H., Chen, Z., Nan, J., Feng, Y., 2014. Improving desalination by coupling membrane capacitive deionization with microbial desalination cell. Desalination 354, 23–29.
WHO (World Health Organization), 2011. Guidelines for Drinking-Water Quality, fourth ed. Chemical Fact Sheets, Geneva (Chapter 12).
Wuana, R.A., Okieimen, F.E., 2011. Heavy metals in contaminated Soils: a Review of sources, chemistry, risks and best available strategies for remediation. ISRN 1–20.

Yang, E., Choi, M.J., Kim, K.Y., Chae, K.J., Kim, I.S., 2015. Effect of initial salt concentrations on cell performance and distribution of internal resistance in microbial desalination cells. Environ. Technol. 36, 852–860.
Yılmaz, A.E., Boncukoğlu, R., Kocakerim, M.M., Yılmaz, M.T., Paluluoğlu, C., 2008. Boron removal from geothermal waters by electrocoagulation. J. Hazard Mater. 153, 146–151.
Yılmaz, A.E., Boncukcuoglu, R., Kocakerim, M.M., 2007. A quantitative comparison between electrocoagulation and chemical coagulation for boron removal from boron-containing solution. J. Hazard Mater. 149, 475–481.